ROYAL SOCIETY OF CHEMISTRY

PAPER

Check for updates

Dinuclear zwitterionic silver(I) and gold(I) complexes bearing 2,2-acetate-bridged bisimidazolylidene ligands†

Bruno Dominelli,[a] Gerri M. Roberts,[a] Christian Jandl,[a] Pauline J. Fischer,[a] Robert M. Reich, [ID][a] Alexander Pöthig, [ID][a] João D. G. Correia [ID][b] and Fritz E. Kühn [ID] *[a]

Four novel dinuclear Ag(I) and Au(I) NHC complexes bearing two 2,2-acetate-bridged bisimidazolylidene ligands (R = Me and iPr) of zwitterionic and metallacyclic forms are reported. The functionalized methylene bridge of the ligands leads to water soluble complexes, which have been characterized by NMR and IR spectroscopy, elemental analysis and single crystal X-ray diffraction in the case of **La-H₂-PF₆**, **Ag₂(La)₂**, **Ag₂(Lb)₂** and **Au₂(La)₂**. Dimerization processes caused by hydrogen bonding or Ag(I)-carboxylate interactions in the solid state were observed for **La-H₂-PF₆** and **Ag₂(La)₂**. DOSY NMR experiments confirmed that both bisimidazolium salts appear as dimers in aqueous solutions, in contrast to the corresponding monomeric Ag(I) and Au(I) complexes. Both gold(I) complexes form *syn*- and *anti*-isomers analogous to the reference coinage metal-based complexes. Protonation studies of the *syn*-isomer gold(I) complex **Au₂(La)₂** were successful, whereas post-modification esterification or amidation reactions were not feasible. Additionally, decarboxylation reactions (thermally induced Krapcho- or oxidative Hunsdiecker-type) of the bisimidazolium salts were observed. Thus, the proximity of the carboxyl moiety to imidazolium/imidazolylidene rings seems to negatively affect stability and reactivity.

Introduction

N-Heterocyclic carbene (NHC) ligands are highly relevant in the design of organometallic compounds for catalysis or medicinal chemistry.[1–3] NHCs are – at least in part – replacing the well-established phosphine-type ligands due to stronger bonding to transition metals, higher versatility and lower toxicity.[4–6] In particular, multidentate NHC ligands give very stable transition metal complexes due to their chelating effect.[7] For example, gold(I), bidentate scaffolds tend to form stable multinuclear complexes in a metallacyclic fashion attributed to the favored linear coordination geometry of coinage metals.[8,9] The historical development and current progress of this class of coinage metal-based complexes were

extensively discussed in a recent review.[9] The stability of these gold(I)-based macrocycles allows in some cases to moderate the reactivity towards thiol groups ensuring a cytotoxic effect without decomposition by blood transport systems (*e.g.* glutathione, serum albumin).[10,11] Another relevant aspect relates to the formation of aurophilic interactions resulting in luminescence properties.[12–14] The proximity of the gold nuclei can be synthetically regulated depending on the type of *N*-substituent, bridging molecules or on the environment (*e.g.* counteranion). Additionally, the coordination sphere of both gold(I) nuclei can be extended under oxidizing conditions (SOCl₂, Br₂ or I₂) by forming for example metallacycles containing Au(I)/Au(III) or even Au(II)/Au(II) with additional coordination of halides.[15,16] Besides the variation of backbone- and *N*-substituents or tuning the flexibility of the bridge, the functionalization of the bridging unit plays an increasingly important role in the design of bidentate NHC moieties.[17] However, the number of bridged-functionalized bidentate NHC ligands and corresponding metal complexes is still limited.[7,17–23] One of the first examples was a palladium(II) complex bearing a 2-hydroxyethane-1,1-diyl-bridged bisimidazolylidene ligand, which has been successfully anchored on styrene functionalized silica and applied in cross coupling catalysis.[17] The presence of a hydroxyl substituent on the

[a]Catalysis Research Center, Molecular Catalysis, Technische Universität München, Ernst-Otto-Fischer-Straße 1, D-85748 Garching bei München, Germany. E-mail: fritz.kuehn@ch.tum.de; Fax: +4989 289 13473; Tel: +49 89 289 13096
[b]Centro de Ciências e Tecnologias Nucleares, Departamento de Engenharia e Ciências Nucleares, Instituto Superior Técnico, Universidade de Lisboa, Campus Tecnológico e Nuclear, Estrada Nacional N° 10 (km 139, 7), 2695-066 Bobadela LRS, Portugal
†Electronic supplementary information (ESI) available. CCDC 1942899–1942902. For ESI and crystallographic data in CIF or other electronic format see DOI: 10.1039/c9dt03035b
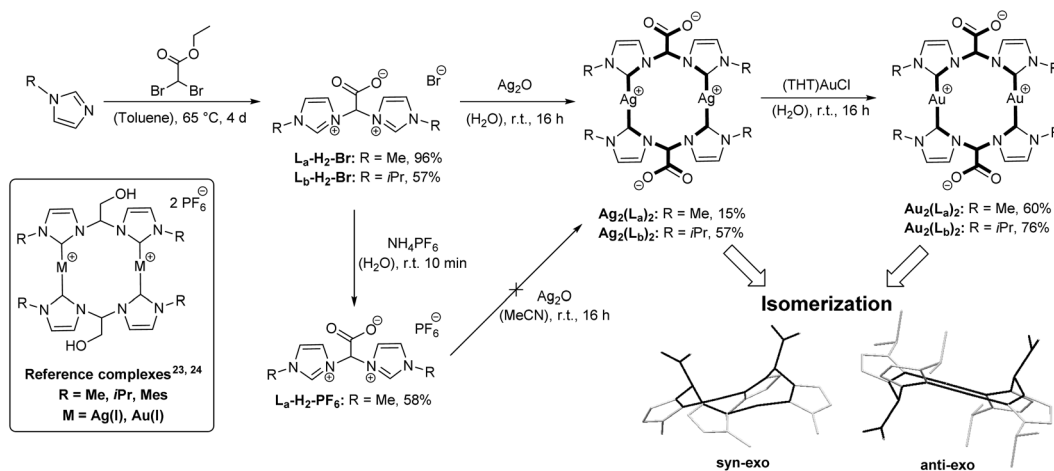
Scheme 1 Synthesis procedure for the bisimidazolium salts $L_{a/b}$-H_2-Br/PF$_6$, silver(I) complexes $Ag_2(L_{a/b})_2$ and the gold(I) complexes $Au_2(L_{a/b})_2$. Additionally, the reference Au(I) complex is depicted.[23,24] Me = methyl, iPr = isopropyl, Mes = mesityl or 2,4,6-trimethylphenyl, THT = tetrahydrothiophen. Both isomer-types, *syn*- and *anti-exo*, are given in the ORTEP-style view of $Ag_2(L_a)_2$ and $Ag_2(L_b)_2$ using capped sticks.((Ortep-style (Oak Ridge thermal ellipsoid plot)).

bridge allows both immobilization and maintenance of the electronic and steric properties given by the backbone and wingtip positions. Dinuclear Cu(I), Ag(I) and Au(I) NHC complexes with the same ligand system have been reported as well. In this family of complexes, the formation of *syn*- and *anti*-isomers, in relation to the methylene bridge, has been observed depending on the metal.[23] More recently, the lipophilic character of the complexes was increased by varying the *N*-substituents. Such a modification led to complexes with moderate antiproliferative activity in the human cancer cell lines HepG2 and A549 (reference complex, Scheme 1).[24] Additionally, the variation of wingtips led to isomer mixtures.

Considering the first results of bridge-functionalized NHC complexes as antiproliferative agents towards cancer cell lines, the abovementioned successive work prompted us to design novel Ag(I) and Au(I) complexes bearing 2,2-acetate bridged bisimidazolylidene for bioconjugation purposes and biological applications.[22,25]

Results and discussion

Synthesis and characterization of ligand precursors

The bisimidazolium salts L_a-H_2-Br and L_b-H_2-Br were synthesized following literature described procedures (Scheme 1).[22,25] The expected ethyl ester group in the bridge could not be obtained due to hydrolysis in the presence of the counter-anion bromide, as reported previously.[22] L_b-H_2-Br requires an additional filtration step over basic aluminium oxide, since it appears in a mixture of carboxylate and carboxylic acid. Another undesired side product identified in the reaction mixture results from the decarboxylation process on the bridge promoted by high temperature. The formation of impurities can be followed by variable temperature ^{1}H-NMR spectroscopy (VT(^{1}H)-NMR, r.t. to 90 °C) as exemplified with

L_a-H_2-Br in DMSO-d$_6$ (Fig. 1). Therefore, to avoid thermal induced decarboxylation on the bridge in solution, the reaction temperature was reduced to 65 °C. Interestingly, when the same experiment was conducted in D$_2$O no decarboxylation was observed. From a mechanistic point of view, a thermally induced Krapcho-type decarboxylation reaction takes places, since the C$_\alpha$ bears electron-withdrawing imidazolium rings.[26] These withdrawing properties additionally explain the isolation of the bisimidazolium salt in the form of carboxylate. Better σ-donating *N*-substituents like isopropyl groups might reduce this effect and indeed, in the case of L_b-H_2-Br, a mixture of carboxylic acid and carboxylate was obtained. Consequently, bisimidazolium derivatives with sterically more demanding *N*-substituents (*e.g.* mesityl, pyridyl, benzyl or *n*-butyl) could not be obtained, since higher reaction temperatures are required. This decarboxylation process could not be
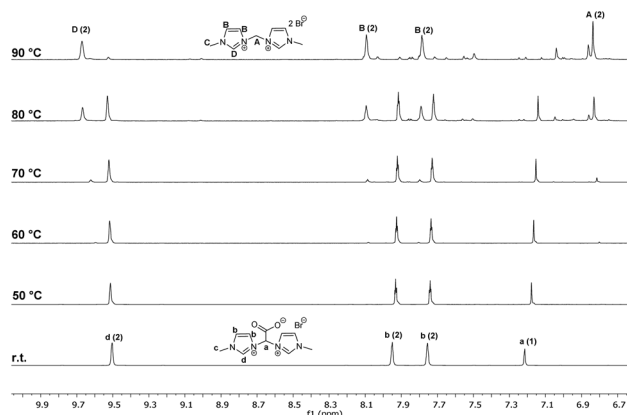

Fig. 1 VT(^{1}H)-NMR (section between 6.5 ppm and 10 ppm) of L_a-H_2-Br in DMSO-d$_6$ between room temperature (r.t.) and 90 °C. The chemical shifts are assigned with letters and the corresponding integral in brackets.

even suppressed by increasing the pressure of a Fischer–Porter bottle with 10 bar CO_2 or the addition of small amounts of water to the aprotic solvents to stabilize the carboxylate group. One of the ways to avoid that process could be, for instance, the elongation of the bridging unit (*e.g.* C_3 or longer) in order to allow the combination of sterically more hindered (more lipophilic) *N*-substituents and a carboxyl group.[25] With the aim of enhancing the solubility in organic solvents, the counter-anion was successfully exchanged in the case of **L$_a$-H$_2$-Br** by adding ammonium hexafluorophosphate (2.5 equivalents) to an aqueous solution of the imidazolium salt. Treatment of the resulting **L$_a$-H$_2$-PF$_6$** with Ag_2O in acetonitrile leads exclusively to the decarboxylated silver(I) complex. Thus, the bromide salt **L$_a$-H$_2$-Br** has proven to be a more suitable ligand precursor than **L$_a$-H$_2$-PF$_6$** for the synthesis of **Ag$_2$(L$_a$)$_2$**, as it displays better water solubility and avoids oxidative decarboxylation.[27]

The imidazolium salts have been characterized by FTIR and multinuclear NMR spectroscopy, elemental analysis and single crystal X-ray diffraction analysis in the case of **L$_a$-H$_2$-PF$_6$**. Suitable crystals of **L$_a$-H$_2$-PF$_6$** were obtained *via* slow diffusion of diethyl ether into a solution of the bisimidazolium salt in acetonitrile. A summary of the crystal data, structure solution, and refinement parameters are given in the ESI† (Table 1). An ORTEP-style view of the zwitterionic molecular structure of **L$_a$-H$_2$-PF$_6$**, together with selected bond lengths and angles are given in Fig. 2.

L$_a$-H$_2$-PF$_6$ crystallizes in the monoclinic space group $P2_1/n$ with three co-crystallized water molecules. No significant differences in bond lengths and angles are observed when comparing this ligand precursor with the previously published hydroxyethyl-2,2-bridged bisimidazolium salt.[17] Five water molecules form a ring by hydrogen bond interactions and consequently connect two bisimidazolium salts in the solid state in the form of a pseudo-dimerization *via* interaction with the carboxylate group. This structural feature could also be confirmed in the FTIR spectrum of **L$_a$-H$_2$-Br**, where two very close peaks assigned to the OH bond stretching and carbonyl stretching were observed.

Synthesis and characterization of Ag(I)-complexes

The zwitterionic Ag(I)-complexes **Ag$_2$(L$_a$)$_2$** and **Ag$_2$(L$_b$)$_2$** were synthesized upon treatment of the respective bisimidazolium salt with Ag_2O in an aqueous solution at room temperature (Scheme 1).[23,24] The water soluble Ag(I)-complexes were characterized by multinuclear NMR and FTIR spectroscopy, elemental analysis and single crystal X-ray diffraction analysis.

Water was observed to co-crystallize in nearly all compounds reported in this work, thus affecting the corresponding elemental analysis by an increased hydrogen content. The functionalization of the bridge with carboxyl groups successfully enhanced the solubility in water introducing four new complexes in the short list reported so far for water-soluble Ag(I)- and Au(I) NHC complexes.[28–35] ORTEP style views of **Ag$_2$(L$_a$)$_2$** and **Ag$_2$(L$_b$)$_2$**, including selected bond lengths and angles, are shown in Fig. 3 and 4, respectively. Single crystals of **Ag$_2$(L$_a$)$_2$** were obtained *via* slow diffusion of acetone into a
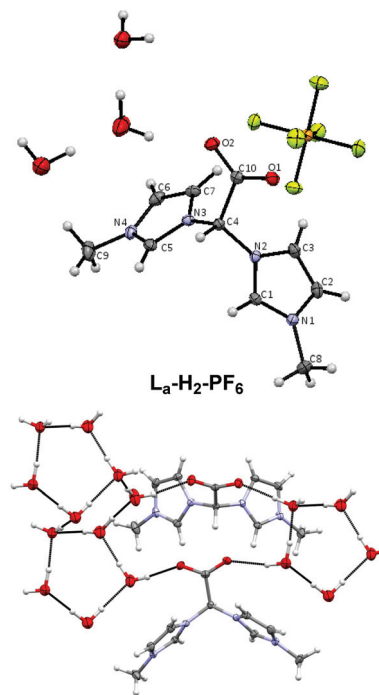

L$_a$-H$_2$-PF$_6$

Fig. 2 ORTEP-style view of the zwitterionic molecular structure of **L$_a$-H$_2$-PF$_6$** with three co-crystallized water molecules (top) and dimerization (bottom). All atoms are shown using ellipsoids at a probability level of 50%. Relevant bond lengths [Å] and angles [°]: N1–C1 1.320(2), N2–C1 1.337(2), N3–C5 1.342(2), N4–C5 1.322(2), N2–C4 1.458(2), N3–C4 1.462(2), C4–C10 1.558(2), C10–O1 1.242(2), C10–O2 1.249(2); N1–C1–N2 108.42(16), N3–C5–N4 108.10(16), N2–C4–N3 111.21(14), C10–C4–N3 112.98(14), C10–C4–N2 112.81(14). O–O distances between carboxylate and water 2.80 Å and the water molecules themselves 2.75 Å (averaged).

solution of the complex in water, crystallizing in the triclinic space group $P\bar{1}$ with 16 co-crystallized water molecules. Suitable crystals of **Ag$_2$(L$_b$)$_2$** were analogously obtained by the slow diffusion of diethyl ether in an ethanol solution and this complex also crystallizes in the triclinic space group $P\bar{1}$ with co-crystallized ethanol molecules. In both cases, all bond lengths and bond angles are similar to the silver reference complex with a hydroxymethyl-functionalized methylene bridge.[24] In particular, the Ag–C bonds are within the range and all C–Ag–C angles are close to the linearity as known for dinuclear, metallacycled Ag(I) NHC complexes of this structure motif. Interestingly, the C–Ag–C angles of **Ag$_2$(L$_b$)$_2$** have a higher linearity when compared to **Ag$_2$(L$_b$)$_2$**. In the case of **Ag$_2$(L$_a$)$_2$** and **Ag$_2$(L$_b$)$_2$**, the distances between both Ag(I) nuclei are 3.60 Å and 3.94 Å, respectively, being not in the range for argentophilic interactions. Such distances are longer than the sum of van der Waals radii (3.4 Å).[36] Accordingly, in comparison with the reference Au(I) complex, the methyl-*N*-substituents lead to a *syn-exo*-isomer (Fig. 3), whereas the isopropyl-wingtips form the anti-*exo* complex (Fig. 4).[24] Interestingly, **Ag$_2$(L$_b$)$_2$** crystallizes in an *anti*-fashion, although this complex was synthesized in aqueous solution and water was expected to regulate the formation of the *syn*-conformation by forming H-bond interactions as observed in complexes of the same type.[23,24]
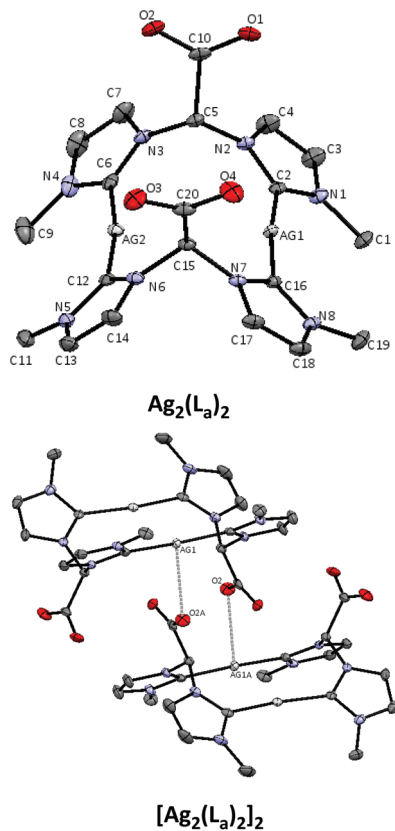
Ag₂(Lₐ)₂

[Ag₂(Lₐ)₂]₂

Fig. 3 ORTEP-style presentation of the zwitterionic molecular structure of **Ag₂(Lₐ)₂** (top) and intermolecular interactions of **[Ag₂(Lₐ)₂]₂** (bottom). All atoms are shown using ellipsoids at a probability level of 50%. H-Atoms and co-crystallized solvents were omitted for clarity. Relevant bond lengths [Å] and angles [°]: Ag1–C2 2.097(2), Ag1–C16 2.102(2), Ag2–C6 2.082(2), Ag2–C12 2.086(2); C2–Ag1–C16 172.01(10), C6–Ag2–C12 171.15(9). Both interactions [Å]: Ag1···O2 2.808(2). Symmetry code to create equivalent atoms: −x, −y, −z.

Intermolecular interactions between the carboxylate group and the Ag(ɪ) nucleus in a T-shape coordination geometry are observed in the case of **Ag₂(Lₐ)₂** (Fig. 3).

Synthesis and characterization of Au(ɪ)-complexes

The gold(ɪ) complexes **Au₂(Lₐ)₂** and **Au₂(L_b)₂** have been synthesized by transmetallation from the corresponding Ag(ɪ) complexes to (THT)AuCl (THT = tetrahydrothiophene) in the aqueous solution.[37] Both water soluble complexes were characterized by multinuclear NMR, FTIR spectroscopy, elemental analysis, and single crystal X-ray diffraction analysis in the case of **Au₂(Lₐ)₂** (Fig. 5). Suitable crystals were obtained *via* slow diffusion of acetone into a solution of **Au₂(Lₐ)₂** in water/ DMSO (1/1). The complex crystallizes in a monoclinic unit cell of *C*2/*m* symmetry. Despite the poor quality, additional co-crystallized acetone and water molecules were detected and water was observed to form hydrogen bond interactions with the carboxylate group probably supporting the formation of the *syn*-isomer. All bond lengths and bond angles, especially the Au–C bonds and the linear C–Au–C angle, are similar to
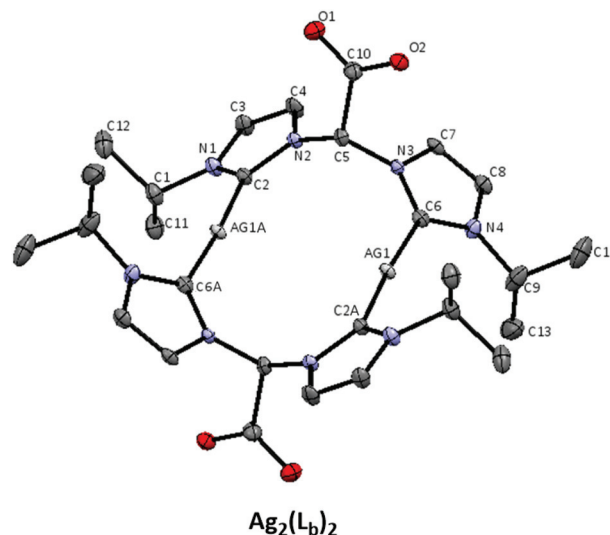
Ag₂(L_b)₂

Fig. 4 ORTEP-style representation of the zwitterionic molecular structure of **Ag₂(L_b)₂**. All atoms are shown using ellipsoids with a probability level of 50%. H-Atoms and co-crystallized solvents were omitted for clarity. Relevant bond lengths [Å] and angles [°]: Ag1–C6 2.086(2), Ag1–C2A 2.087(2), Ag1A–C2 2.087(2), Ag1A–C6A 2.087(2), C6–Ag1–C2A 175.65(9), C2–Ag1A–C6A 175.65(9). Symmetry code to create equivalent atoms: −x, −y, −z.
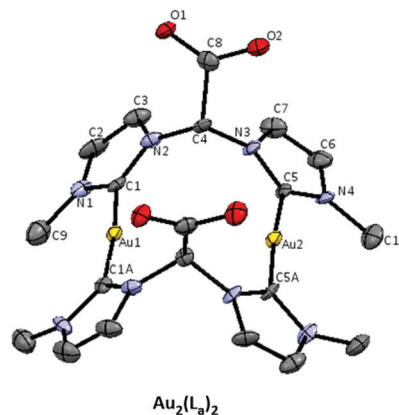
Au₂(Lₐ)₂

Fig. 5 ORTEP-style plot of the zwitterionic molecular structure of **Au₂(Lₐ)₂**. All atoms are shown with thermal ellipsoids of a 50% probability level. H-Atoms and co-crystallized solvents were omitted for clarity. Relevant bond lengths [Å] and angles [°]: Au1–C1 2.013(5), Au1–C1A 2.013(5), Au2–C5 2.012(5), Au2–C5A 2.012(5), C1–Au1–C1A 173.6(3), C5–Au2–C5A 175.1(3). Symmetry code to create equivalent atoms: *x*, 1 − *y*, *z*.

the reference gold complex (Scheme 1).[24] The distance between both Au(ɪ) nuclei (3.77 Å) is not in the range of aurophilic interactions being longer than the sum of van der Waals radii (3.32 Å).[36] Also here, the *syn-exo* isomer was obtained, similarly to the case of the analogue **Ag₂(Lₐ)₂** complex.

The *syn-exo* species precipitates in an isomerically pure manner after the concentration of the aqueous solution. Unlike **Au₂(Lₐ)₂**, **Au₂(L_b)₂** could not be isolated as a single

crystal and thus no XRD structure was obtained. The proton NMR spectrum of $Au_2(L_b)_2$ shows an isomer mixture, displaying an analogue behavior as observed for the hydroxyethyl-2,2-diyl-bridged bismidazolydene gold(I) complex with isopropyl *N*-substituents.

DOSY NMR experiment

In the case of L_a-H_2-PF_6 and $Ag_2(L_a)_2$, a dimerization was observed in the solid state. Consequently, DOSY NMR experiments in D_2O at room temperature were conducted for all bisimidazolium salts reported herein and the corresponding Ag(I) and Au(I) complexes to analyze the structural behavior in solution. All obtained diffusion coefficients and calculated hydrodynamic radii (Stokes equation) are summarized in Table 1.

Table 1 Diffusion coefficient and calculated hydrodynamic radii of L_a-H_2-Br, L_b-H_2-Br, $Ag_2(L_a)_2$, $Ag_2(L_a)_2$, $Ag_2(L_a)_2$ and $Ag_2(L_a)_2$. Stokes equation: $R_0 = (k_b \cdot T)/(6\pi \cdot \eta \cdot D)$. $k_B = 1.38 \times 10^{-23}$ J K^{-1}, $T = 298$ K, $\eta(D_2O) = 0.891 \times 10^{-3}$ Pa s

	Diffusion coefficient D [cm^2 S^{-1}]	Hydrodynamic radius R_0 [Å]
L_a-H_2-Br	4.60×10^{-6}	5.32
L_b-H_2-Br	4.74×10^{-6}	5.17
$Ag_2(L_a)_2$	4.13×10^{-6}	5.93
$Ag_2(L_b)_2$	4.40×10^{-6}	5.56
$Au_2(L_a)_2$	4.26×10^{-6}	5.75
$Au_2(L_b)_2$	4.00×10^{-6}	6.12

Collectively the results obtained demonstrate that also in solution both ligand precursors exist as dimers, since the hydrodynamic radii are in the range of those of the complexes. Comparing the latter value with the profile distances in all three axis *x*, *y* and *z* of the single crystal structure of $Ag_2(L_a)_2$, it is confirmed that no dimerization is observed in the aqueous solution in the case of all four complexes. In the case of $Au_2(L_b)_2$, the DOSY experiment was conducted with the isomer mixtures and both isomers exhibit the same coefficient showing no specific difference in their size in solution.

Reactivity studies

First post-modifications *via* esterification and amidation reactions were conducted on L_a-H_2-Br and on $Au_2(L_a)_2$ in order to find a suitable coupling method of the carboxylate for bioconjugation. A summary of all attempted methods are given in the ESI† (Scheme 1).[38] Unfortunately, neither the activation of the carboxylate (acyl chloride or mixed anhydride) nor the use of coupling reagents led to a successful post-modification. Thereby, isopentylamine or 9-(hydroxymethyl)anthracene was chosen as the coupling reagent to increase the degree of lipophilicity and to insert chromophoric systems. Thus, in addition to being sensitive to decarboxylation, the proximity of the carboxylate group to the imidazolium or imidazolylidene moiety leads to lower reactivity.

Next, the zwitterionic $Au_2(L_a)_2$ and $Au_2(L_b)_2$ were treated with 10 w% of aqueous hydrobromic acid and trifluoro acetic or 2.1
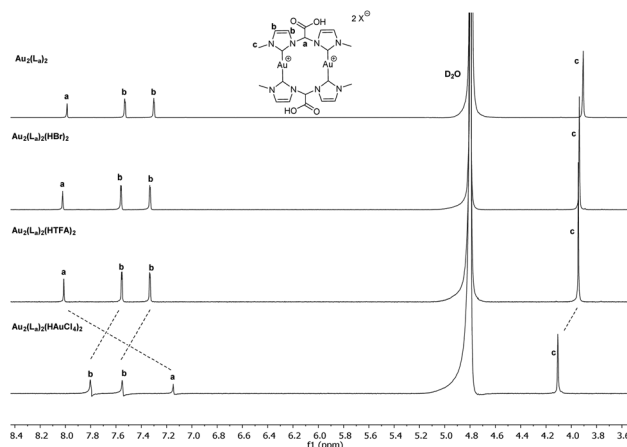

Fig. 6 Stacked ^{1}H NMR spectra in the section of 3.5 ppm and 8.5 ppm of $Au_2(L_a)_2$, $Au_2(L_a)_2(HBr)_2$, $Au_2(L_a)_2(HTFA)_2$ and $Au_2(L_a)_2(HAuCl_4)_2$ in D_2O at room temperature.

equivalents of tetrachloroauric(III) acid. Thereby, the influence of counter-anions on the structure of the complexes, particularly with the additional presence of carboxylic acids, was studied. The approximation of two Au(I) nuclei until aurophilic interactions in similar metallacyclic systems have been reported after re-salination to bromide.[13] In the case of $Au_2(L_a)_2$, all protonated products, $Au_2(L_a)_2(HBr)_2$, $Au_2(L_a)_2(HTFA)_2$ and $Au_2(L_a)_2(HAuCl_4)_2$ precipitated in the aqueous solution after the addition of the corresponding acidic solution and could be characterized by NMR spectroscopy and elemental analysis. In the proton spectra (Fig. 6), no changing chemical shift patterns are observed for $Au_2(L_a)_2(HBr)_2$ and $Au_2(L_a)_2(HTFA)_2$ when compared to the starting zwitterionic $Au_2(L_a)_2$ indicating no structural diversity of the protonated products.

Interestingly, the resonance pattern of $Au_2(L_a)_2(HAuCl_4)_2$ changed, since the proton of the methylene bridge is shifted to a high field (~1 ppm). A direct interaction of a halide with the methylene-H-atom should lead to a downfield shift, as previously reported.[13] Thus, the interaction presumably occurs between the carboxylic acid and the tetrachloroaurate(III) counter-anion, which formally discharges the bridging proton causing the highfield shift. Additionally, the CH$_3$-group shifts downfield indicating a possible enhancement of strain in the metallacycle. Nevertheless, related to the elemental analysis a mixed-valent tetranuclear gold(I/III) complex could be isolated after the use of a metal-based acid.

In the case of $Au_2(L_b)_2$, which is expected to crystallize in analogy to the reference complex as the *anti-exo* isomer (Scheme 1), it immediately decomposes after the addition of each of the three acids, indicating the lower stability of the *anti*-isomer compared to the *syn*-species.

Conclusions

The 2,2-acetate-bridged bisimidazolium salts L_a-H_2-Br/PF_6 and L_b-H_2-Br,[22,25] allow the preparation of the zwitterionic com-

plexes **Ag₂(Lₐ)₂**, **Ag₂(L_b)₂**, **Au₂(Lₐ)₂** and **Au₂(L_b)₂**. The obtained compounds have been characterized by NMR and FTIR spectroscopy, elemental analysis and single crystal X-ray diffraction in the case of **Lₐ-H₂-PF₆**, **Ag₂(Lₐ)₂**, **Ag₂(L_b)₂** and **Au₂(Lₐ)₂**. Hydrogen bond interactions between the carboxylate group and co-crystallized water molecules were observed in the single crystal structure of **Lₐ-H₂-PF₆**, indicating a pseudo-dimerization process in the solid state caused by the five-membered ring of water molecules. DOSY experiments of **Lₐ-Hₐ-Br** and **L_b-H₂-Br** allowed the determination of the respective diffusion coefficients, which are similar to those of the corresponding Ag(I) and Au(I) complexes. Consequently, both ligand precursors are expected to behave as dimers in solution. **Ag₂(Lₐ)₂** crystallizes in the *syn*-form, whereas **Ag₂(L_b)₂** crystallizes as the *anti*-isomer, being similar to the analogous reference system.[24] **Ag₂(Lₐ)₂** shows intermolecular coordinative interactions in a T-shape between the carboxylate group and one of the Ag(I) atoms of a neighboring complex, leading again to a dimer in the solid state. DOSY experiments on the complexes reveal hydrodynamic radii in the same range as observed for the monomeric structure. The presence of a carboxyl group at the bridging unit promotes water solubility. The proximity of the carboxylate group to imidazolium/imidazolylidene rings leads to thermally induced Krapcho-type or oxidative Hunsdiecker-type decarboxylation. Performing the synthesis in water suppresses the undesired decarboxylation. Additionally, the carboxylate group is unreactive towards esterification or amidation routes complicating the post-modification for bio-conjugation. The complex **Au₂(Lₐ)₂** was successfully protonated with various acids leading to the products **Au₂(Lₐ)₂(HBr)₂**, **Au₂(Lₐ)₂(HTFA)₂** and **Au₂(Lₐ)₂(HAuCl₄)₂**. **Au₂(L_b)₂**, expected to crystallize in the *anti*-form decomposes under acidic conditions. In the case of **Au₂(Lₐ)₂(HAuCl₄)₂**, the resonance pattern in the ¹H NMR spectrum extremely differs when compared to **Au₂(Lₐ)₂**, which is explained by interactions with the counter-anion and enhanced ring tension of the metallacycle. This protonation method allows access to mixed-valent Au(I/III) complexes consisting of cationic and anionic components. **Au₂(L_b)₂** immediately decomposes under acidic conditions showing a higher stability of the *syn-exo* isomer than the *anti-exo* species.

Experimental

Synthesis of bisimdazolium salts

Lₐ-H₂-Br: 2,2-Dibromo acetate ethyl ester (5.26 mL, 10.0 g, 40.7 mmol, 1.0 eq.) and 1-methylimidazole (13.0 mL, 13.4 g, 162.7 mmol, 4.0 eq.) are dissolved in toluene (15 mL and stirred for 4 days at 65 °C. The brown precipitate is separated by vacuum filtration and washed 3× with toluene (5 mL), 3× with acetonitrile (5 mL) and finally 3× with diethyl ether (5 mL). The white solid is dissolved in methanol, stirred in basic aluminium oxide for 30 min and after filtration re-precipitated with diethyl ether. After drying under dynamic vacuum, 11.8 g of **Lₐ-H₂-Br** as a white powder is obtained. Yield: 96%.

¹H NMR (400 MHz, DMSO-d_6, 300 K): δ 9.53–9.44 (m, 2H, NCHN), 7.92 (t, 2H, J_{HH} = 1.8 Hz, NCHCHN), 7.74 (t, 2H, J_{HH} = 1.8 Hz, NCHCHN), 7.16 (s, 1H, NCH(COO)N), 3.89 (s, 6H, CH_3). ¹H NMR (400 MHz, D₂O, 300 K): δ 7.73 W(t, 2H, J_{HH} = 1.8 Hz, NCHCHN), 7.56 (t, 2H, J_{HH} = 1.8 Hz, NCHCHN), 3.94 (m, 6H, CH_3).¹³C NMR (101 MHz, DMSO-d₆, 300 K): δ 159.35 (CHCOO), 137.82 (NCHN), 123.44 (NCHCHN), 121.92 (NCHCHN), 70.41 (NCH(COO)N), 36.06 (CH₃). EA calcd: C 35.62, H 5.08, N 16.62. Found: C 35.56, H 4.89, N 16.32. **FT-IR** (cm⁻¹): 3384 (OH), 3444 (OH), 1662 (C=O), 1678 (C=O).

L_b-H₂-Br: The same procedure as that of **Lₐ-H₂-Br** using 2,2-dibromo acetate ethyl ester (5.26 mL, 10.0 g, 40.7 mmol, 1.0 eq.) and 1-isopropylimidazole (18.5 mL, 17.9 g, 162.7 mmol, 4.0 eq.) in toluene (15 mL). 8.3 g of the desired product as a white powder is obtained. Yield: 57%.

¹H NMR (400 MHz, DMSO-d_6, 300 K): δ 9.62 (d, 2H, J_{HH} = 1.9 Hz NCHN), 8.04–8.01 (m, 2H, NCHCHN), 7.99–7.97 (m, 2H, NCHCHN), 7.13 (s, 1H, NCH(COO)N), 4.70 (p, 2H, J_{HH} = 6.7 Hz, CH(CH₃)₂), 1.49 (dd, 12H, J_{HH} = 6.5 Hz, J_{HH} = 3.2 Hz, CH_3). ¹H NMR (400 MHz, D₂O, 300 K): δ 7.81 (dd, 2H, J_{HH} = 2.1 Hz, 1.0 Hz, NCHCHN), 7.76 (d, 2H, J_{HH} = 2.2 Hz, NCHCHN), 4.73 (h, 2H, J_{HH} = 6.7 Hz, CH(CH₃)₂), 1.59 (d, 12H, J_{HH} = 6.7 Hz, CH_3). ¹³C NMR (101 MHz, DMSO-d₆, 300 K): δ 159.40 (CHCOO), 136.19 (NCHN), 122.38 (NCHCHN), 120.33 (NCHCHN), 70.52 (NCH(COO)N), 52.64 (CH(CH₃)₂), 22.17 (CH₃), 22.05 (CH₃). FT-IR (cm⁻¹), 3436 (OH), 1674 (C=O).

Synthesis of silver(I)-bis(NHC) complexes

Ag₂(Lₐ)₂: **Lₐ-H₂-Br** (1.0 g, 3.3 mmol, 1.0 eq.) and Ag₂O (1.9 g, 8.3 mmol, 2.5 eq.) are suspended in water (50 mL) and stirred at room temperature for 16 h under exclusion of light. The brown suspension is centrifuged and filtered over Celite®. The resulting colourless solution is concentrated *in vacuo* and **Ag₂(Lₐ)₂** is obtained as a white solid *via* repeated fractional precipitation with acetone. The precipitate is washed 3× with acetone (5 mL) and diethyl ether, respectively. 155 mg of **Ag₂(Lₐ)₂** is obtained. Yield: 15%.

¹H NMR (400 MHz, D₂O, 300 K): δ 7.51 (d, 4H, J_{HH} = 1.9 Hz, NCHCHN), 7.48 (s, 2H, NCH(COO)N), 7.28 (d, 4H, J_{HH} = 1.9 Hz, NCHCHN), 3.86 (s, 12H, CH_3). ¹³C NMR (101 MHz, D₂O, 300 K): δ 183.09 (NCN), 169.70 (COO), 124.75 (NCHCHN), 120.99 (NCHCHN), 39.28 (CH₃), NCH(COO)N not visible. EA calcd with 1.15 H₂O: C 35.59, H 3.63, N 16.60. Found: C 35.08, H 3.34, N 15.85. **FT-IR** (cm⁻¹): 1636 (C=O).

Ag₂(L_b)₂: The same procedure as that of **Ag₂(Lₐ)₂** using **L_b-H₂-Br** (1.0 g, 2.8 mmol, 1.0 eq.) and Ag₂O (1.62 g, 7.0 mmol, 2.5 eq.) in water (50 mL). 0.70 g of the desired product as a white powder is obtained. Yield: 57%.

¹H NMR (400 MHz, D₂O, 300 K): δ 7.57 (d, 4H, J_{HH} = 2.3 Hz, NCHCHN), 7.54 (s, 2H, NCH(COO)N), 7.41 (d, 4H, J_{HH} = 2.0 Hz, NCHCHN), 4.64 (p, 4H, J_{HH} = 6.7 Hz, CH(CH₃)₂), 1.42 (d, 12H, J_{HH} = 6.7 Hz, CH_3), 1.28–1.21 (m, 12H, J_{HH} = 6.7 Hz, CH_3). ¹³C NMR (101 MHz, D₂O, 300 K): δ 168.58 (COO), 119.67 (NCHCHN), 54.48 (CH(CH₃)₂) 22.88 (CH₃) 22.65 (CH₃), NCN, NCHCHN and NCH(COO)N not visible. EA calcd with 2 H₂O: C

41.91, H 5.28, N 13.96. Found: C 41.20, H 5.43, N 13.54. **FT-IR** (cm^{-1}): 3405 (OH), 1651 (C=O).

Synthesis of gold(I)-bis(NHC) complexes

Au$_2$(L$_a$)$_2$: Ag$_2$(L$_b$)$_2$ (0.12 g, 0.19 mmol, 1.0 eq.) and (tetrahydrothiophene)gold(I)chloride (0.13 g, 0.39 mmol, 2.1 eq.) are suspended in water (50 mL) and stirred at room temperature for 16 h under exclusion of light. The suspension is centrifuged and vacuum-filtered. The resulting colourless solution is concentrated *in vacuo* and **Au$_2$(L$_a$)$_2$** crystallizes as a white powder after storage at 4 °C. The precipitate is washed 3× with acetone (5 mL) and diethyl ether, respectively and dried under dynamic vacuum. 90 mg of **Au$_2$(L$_a$)$_2$** is obtained. Yield: 60%.

^{1}H NMR (400 MHz, D$_2$O, 300 K): *syn*-isomer δ 7.99 (s, 2H, NC*H*(COO)N), 7.53 (d, 4H, J_{HH} = 2.1 Hz, NC*H*CHN), 7.30 (d, 4H, J_{HH} = 2.1 Hz, NCHC*H*N), 3.91 (s, 12H, C*H*$_3$). ^{13}C Cryo NMR (101 MHz, D$_2$O, 300 K): δ 185.01 (N*C*N), 167.87 (*C*OO), 124.33 (N*C*HCHN), 119.70 (NCH*C*HN), 74.54 (N*C*H(COO)N), 37.59 (*C*H$_3$). EA calcd with 1 H$_2$O: C 28.25, H 2.84, N 13.18. Found: C 28.27, H 2.76, N 13.15. **FT-IR** (cm^{-1}): 1651 (C=O).

Au$_2$(L$_b$)$_2$: The same procedure as that of **Au$_2$(L$_a$)$_2$** using Ag$_2$(L$_b$)$_2$ (0.05 g, 0.07 mmol, 1.0 eq.) and (tetrahydrothiophene)gold(I)-chloride (0.044 g, 0.14 mmol, 2.1 eq.) suspended in water (10 mL) and stirred at room temperature for 16 h under exclusion of light. The suspension is centrifuged, vacuum-filtered and water is completely removed *in vacuo*. The desired product is obtained after repeated fractional precipitation with ethanol and diethyl ether in the second fraction. The precipitate is washed 3× with diethyl ether (5 mL) and dried under dynamic vacuum. 0.05 g is obtained as a white powder. Yield: 76%.

^{1}H NMR (400 MHz, D$_2$O, 300 K): *anti*-isomer δ 7.90 (s, 2H, NC*H*(COO)N), 7.53 (d, 4H, J_{HH} = 2.5 Hz, NC*H*CHN), 7.43 (d, 4H, J_{HH} = 1.9 Hz, NCHC*H*N), 4.89–4.82 (m, 4H, C*H*(CH$_3$)$_2$), 1.46–1.42 (m, 12H, C*H*$_3$), 1.28 (dd, 12H, J_{HH} = 6.4 Hz, 2.2 Hz, C*H*$_3$). ^{13}C NMR (101 MHz, D$_2$O, 300 K): δ 183.36 (N*C*N), 167.65 (*C*OO), 120.08 (N*C*HCHN), 119.61 (NCH*C*HN), 75.37 (N*C*H(COO)N) 53.99 (*C*H(CH$_3$)$_2$), 22.66 (*C*H$_3$), 22.09 (*C*H$_3$). EA calcd with 2 H$_2$O: C 34.30, H 4.32, N 11.43. Found: C 33.22, H 4.24, N 10.90. **FT-IR** (cm^{-1}): 3384 (OH), 1664 (C=O).

Decarboxylation studies

In a NMR scale experiment, 5 mg of the analyzed compound is dissolved in 0.45 mL of the corresponding deuterated solvent and after being heated for 10 min proton NMR is measured at the adjusted temperature (r.t. until 90 °C).

Protonation studies

Au$_2$(L$_a$)$_2$(HBr)$_2$: To a solution of **Au$_2$(L$_a$)$_2$** (10.0 mg, 12.0 μmol, 1.0 eq.) in water (3.5 mL) is added a 10 w% aqueous hydro bromic acid solution (0.50 mL) and stirred for 10 min at room temperature. The white precipitate is isolated by centrifugation, washed 3× with water (0.50 mL) and dried under dynamic vacuum. 4 mg of **Au$_2$(L$_a$)$_2$(HBr)$_2$** is obtained as a white powder. Yield: 33%.

^{1}H NMR (400 MHz, D$_2$O, 300 K): δ 8.01 (s, 2H, NC*H*(COO)N), 7.55 (d, 4H, J_{HH} = 2.1 Hz, NC*H*CHN), 7.32 (d, 4H, J_{HH} = 2.1 Hz, NCHC*H*N), 3.93 (s, 12H, C*H*$_3$). EA calcd: C 24.16, H 2.43, N 11.27. Found: C 23.15, H 2.57, N 10.64.

Au$_2$(L$_a$)$_2$(HTFA)$_2$: The same procedure as that of **Au$_2$(L$_a$)$_2$(HBr)$_2$**. Yield: 7%.

^{1}H NMR (400 MHz, D$_2$O, 300 K): δ 8.01 (s, 2H, NC*H*(COO)N), 7.55 (d, 4H, J_{HH} = 2.1 Hz, NC*H*CHN), 7.32 (d, 4H, J_{HH} = 2.1 Hz, NCHC*H*N), 3.94 (s, 12H, C*H*$_3$). EA calcd: C 27.08, H 2.91, N 10.53. Found: C 26.45, H 3.23, N 8.42.

Au$_2$(L$_a$)$_2$(HAuCl$_4$)$_2$: To a solution of **Au$_2$(L$_a$)$_2$** (10.0 mg, 12.0 μmol, 1.0 eq.) in water (3.5 mL) is added tetrachloroauric acid (8.57 mg, 25.2 μmol, 2.1 eq.) in water (2 mL) and an analogue procedure to that of **Au$_2$(L$_a$)$_2$(HBr)$_2$** is adopted. Yield: 47%.

^{1}H NMR (400 MHz, D$_2$O, 300 K): δ 7.79 (d, 4H, J_{HH} = 2.0 Hz, NC*H*CHN), 7.54 (d, 4H, J_{HH} = 2.0 Hz, NCHC*H*N), 7.13 (s, 2H, NC*H*(COO)N), 4.10 (s, 12H, C*H*$_3$). EA calcd: C 15.89, H 1.60, N 7.41. Found: C 14.81, H 1.76, N 6.82.

Conflicts of interest

There are no conflicts to declare.

Acknowledgements

References

1 M. N. Hopkinson, C. Richter, M. Schedler and F. Glorius, *Nature*, 2014, **510**, 485–496.

2 J. A. M. Lummiss, C. S. Higman, D. L. Fyson, R. McDonald and D. E. Fogg, *Chem. Sci.*, 2015, **6**, 6739–6746.

3 W. K. Liu and R. Gust, *Coord. Chem. Rev.*, 2016, **329**, 191–213.

4 B. Dominelli, J. D. G. Correia and F. E. Kühn, *J. Organomet. Chem.*, 2018, **866**, 153–164.

5 M. Mora, M. C. Gimeno and R. Visbal, *Chem. Soc. Rev.*, 2019, **48**, 447–462.

6 P. F. Ai, C. Gourlaouen, A. A. Danopoulos and P. Braunstein, *Inorg. Chem.*, 2016, **55**, 1219–1229.

7 A. C. Lindhorst, M. Kaspar, P. J. Altmann, A. Pöthig and F. E. Kühn, *Dalton Trans.*, 2018, **47**, 1857–1867.

8 M. Porchia, M. Pellei, M. Marinelli, F. Tisato, F. Del Bello and C. Santini, *Eur. J. Med. Chem.*, 2018, **146**, 709–746.

9   M. M. Gan, J. Q. Liu, L. Zhan, Y. Y. Wang, F. E. Hahn and Y. F. Han, *Chem. Rev.*, 2018, **118**, 9587–9641.

10 T. Zou, C.-N. Lok, P.-K. Wan, Z.-F. Zhang, S.-K. Fung and C.-M. Che, *Curr. Opin. Chem. Biol.*, 2018, **43**, 30–36.

11 T. Zou, C. T. Lum, C. N. Lok, W. P. To, K. H. Low and C. M. Che, *Angew. Chem., Int. Ed.*, 2014, **53**, 5810–5814.

12 C. Hemmert, R. Poteau, F. Dominique, P. Ceroni, G. Bergamini and H. Gornitzka, *Eur. J. Inorg. Chem.*, 2012, 3892–3898.

13 A. A. Penney, V. V. Sizov, E. V. Grachova, D. V. Krupenya, V. V. Gurzhiy, G. L. Starova and S. P. Tunik, *Inorg. Chem.*, 2016, **55**, 4720–4732.

14 T. P. Pell, B. D. Stringer, C. Tubaro, C. F. Hogan, D. J. D. Wilson and P. J. Barnard, *Eur. J. Inorg. Chem.*, 2017, 3661–3674.

15 M. Baron, M. Dalla Tiezza, A. Carlotto, C. Tubaro, C. Graiff and L. Orian, *J. Organomet. Chem.*, 2018, **866**, 144–152.

16 A. H. Mageed, B. W. Skelton, A. N. Sobolev and M. V. Baker, *Eur. J. Inorg. Chem.*, 2018, 109–120.

17 R. Zhong, A. Pöthig, S. Haslinger, B. Hofmann, G. Raudaschl-Sieber, E. Herdtweck, W. A. Herrmann and F. E. Kühn, *ChemPlusChem*, 2014, **79**, 1294–1303.

18 O. Kühl, *Germany Pat*, WO2012034880A1, 2012.

19 E. Mas-Marzá, M. Poyatos, M. Sanaú and E. Peris, *Organometallics*, 2004, **23**, 323–325.

20 E. Mas-Marzá, M. Sanaú and E. Peris, *J. Organomet. Chem.*, 2005, **690**, 5576–5580.

21 M. Viciano, E. Mas-Marzá, M. Poyatos, M. Sanaú, R. H. Crabtree and E. Peris, *Angew. Chem., Int. Ed.*, 2005, **44**, 444–447.

22 R. Puerta-Oteo, M. Hölscher, M. V. Jiménez, W. Leitner, V. Passarelli and J. J. Pérez-Torrente, *Organometallics*, 2018, **37**, 684–696.

23 R. Zhong, A. Pöthig, D. C. Mayer, C. Jandl, P. J. Altmann, W. A. Herrmann and F. E. Kühn, *Organometallics*, 2015, **34**, 2573–2579.

24 J. Rieb, B. Dominelli, D. Mayer, C. Jandl, J. Drechsel, W. Heydenreuter, S. A. Sieber and F. E. Kühn, *Dalton Trans.*, 2017, **46**, 2722–2735.

25 Y. Li, B. Dominelli, R. M. Reich, B. Liu and F. E. Kühn, *Catal. Commun.*, 2019, **124**, 118–122.

26 A. P. Krapcho, J. F. Weimaster, J. M. Eldridge, E. G. E. Jahngen, A. J. Lovey and W. P. Stephens, *J. Org. Chem.*, 1978, **43**, 138–147.

27 R. G. Johnson and R. K. Ingham, *Chem. Rev.*, 1956, **56**, 219–269.

28 C. E. Czegeni, G. Papp, A. Katho and F. Joo, *J. Mol. Catal. A: Chem.*, 2011, **340**, 1–8.

29 E. Tomas-Mendivil, P. Y. Toullec, J. Borge, S. Conejero, V. Michelet and V. Cadierno, *ACS Catal.*, 2013, **3**, 3086–3098.

30 H. Ibrahim, P. de Fremont, P. Braunstein, V. Thery, L. Nauton, F. Cisnetti and A. Gautier, *Adv. Synth. Catal.*, 2015, **357**, 3893–3900.

31 G. A. Fernandez, A. B. Chopa and G. F. Silbestri, *Catal. Sci. Technol.*, 2016, **6**, 1921–1929.

32 Ö. Karaca, V. Scalcon, S. M. Meier-Menches, R. Bonsignore, J. Brouwer, F. Tonolo, A. Folda, M. P. Rigobello, F. E. Kühn and A. Casini, *Inorg. Chem.*, 2017, **56**, 14237–14250.

33 M. Pellei, V. Gandin, M. Marinelli, C. Marzano, M. Yousufuddin, H. V. R. Dias and C. Santini, *Inorg. Chem.*, 2012, **51**, 9873–9882.

34 P. C. Kunz, C. Wetzel, S. Kogel, M. U. Kassack and B. Spingler, *Dalton Trans.*, 2011, **40**, 35–37.

35 G. A. Fernandez, A. S. Picco, M. R. Ceolin, A. B. Chopa and G. F. Silbestri, *Organometallics*, 2013, **32**, 6315–6323.

36 A. Bondi, *J. Phys. Chem.*, 1964, **68**, 441–451.

37 J. Cure, R. Poteau, I. C. Gerber, H. Gornitzka and C. Hemmert, *Organometallics*, 2012, **31**, 619–626.

38 C. Montalbetti and V. Falque, *Tetrahedron*, 2005, **61**, 10827–10852.